Simulation of a Parametric Resonance Circuit

Franklin D. Amador*, Horst Eckardt†
A.I.A.S. and UPITEC
(www.aias.us, www.atomicprecision.com, www.upitec.org)

March 30, 2012

Abstract

Special resonance circuits are investigated with circuit elements being parametric, i.e. variable in time. It is shown by simulation that energy from spacetime is possible in certain cases. A variable capacitance can give rise to giant oscillations, widely exceeding the limit of classical resonance theory. The resonance can be limited to final values by a special design, making such devices relatively easy to construct.

Keywords: resonance, electrical circuit, damped resonance circuit, parametric circuit, electrodynamics simulation

1 Introduction

History has shown that power generation technology has progressed in the following steps; 1) Mechanical: by physical labor or machines, 2) Chemical: by steam or re-combination of Hydrogen (H) & Oxygen (O) from either *water* or fossil fuels, 3) Subatomic: by the exploitations in natures imbalances of certain elements, and 4) Electromagnetic: by moving magnetic fields over wires to produce voltage and current. Each step an obvious improvement of the latter and all with a basic principle in common - Resonance.

At AIAS we further define this basic principle as "Spin Connection Resonance"(SCR [1]). The mechanical versions of parametric elements $(L(t), C(t), R(t))$ are usually driven so that their parameter changes in relation to the rotational speed (rpm) of an electric motor. When these parametric element values are in "consonance" to the resonant behavior of the rest of the circuit then we have achieved SCR [1].

In this paper, we will study existing electromagnetic power generation [3] with emphasis on the solid state version of the mechanical parametric circuits. What we find is that parametric circuits transfers energy in the time domain by drawing energy at one frequency and supplying energy at another frequency [6].

*email: fdamador@comcast.net
†email: horsteck@aol.com

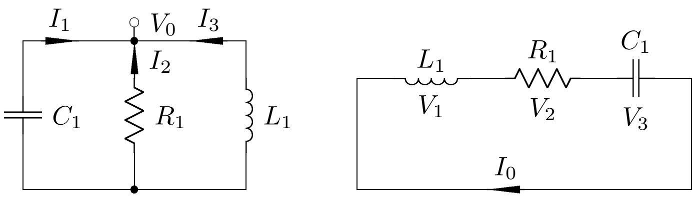

Figure 1: Parallel & Series Circuit.

Additionally, we find that the energy transfered is dependent on the rate-of-change of the parametric element at 1) $\frac{d}{dt}$, 2) $\frac{d^2}{dt^2}$ [7] [8], and higher 3) $\frac{d^n}{dt^n}$. This reveals that if the non-linear element $(L(t), C(t), R(t))$ is driven faster in time, then additional power $(Joules/seconds)$ can be drawn in from the time domain at a rate higher than what the circuit can release as heat; thus, producing available and useful power for additional loads.

2 Resonance in Circuits

In this section we discuss static (conventional) and parametric (time-varying, dynamic) resonances.

2.1 Principles of Resonance in Static Circuit

First of all, let's study the current resonance in standard circuit analysis. For instance, circuits with Resistance (R), Inductance (L) and Capacitance (C) elements in a single network will result in second-order differential equations [9] [10] [11]. Figure 1 shows the two basic parallel and series second order circuits.

Using the node voltage method for the parallel circuit and Kirchhoff's voltage law for the series circuit our analysis gives:

$$\begin{array}{cc} Parallel & Series \\ I_1 + I_2 + I_3 = 0 & V_1 + V_2 + V_3 = 0 \end{array} \tag{1}$$

Now, with the proper substitution of elements shown below

$$\begin{array}{cc} Parallel & Series \\ I_1 = C_1 \frac{dV_0}{dt} & V_1 = L_1 \frac{dI_0}{dt} \end{array} \tag{2}$$

$$I_2 = \frac{V_0}{R_1} \qquad V_2 = R_1 I_0 \tag{3}$$

$$I_3 = \frac{1}{L_1} \int V_0 dt \qquad V_3 = \frac{1}{C_1} \int I_0 dt \tag{4}$$

we end up with,

$$C_1 \frac{dV_0}{dt} + \frac{V_0}{R_1} + \frac{1}{L_1} \int V_0 dt = 0 \qquad L_1 \frac{dI_0}{dt} + R_1 I_0 + \frac{1}{C_1} \int I_0 dt = 0 \tag{5}$$

now, for parallel we divide by C_1 and for series by L_1,

$$\frac{dV_0}{dt} + \frac{1}{R_1C_1}V_0 + \frac{1}{L_1C_1}\int V_0 dt = 0 \qquad \frac{dI_0}{dt} + \frac{R_1}{L_1}I_0 + \frac{1}{L_1C_1}\int I_0 dt = 0 \quad (6)$$

and finally we differentiate with respect to time d/dt.

$$\frac{d^2V_0}{d^2t} + \frac{1}{R_1C_1}\frac{dV_0}{dt} + \frac{1}{L_1C_1}V_0 = 0 \qquad \frac{d^2I_0}{d^2t} + \frac{R_1}{L_1}\frac{dI_0}{dt} + \frac{1}{L_1C_1}I_0 = 0 \quad (7)$$

Lastly, we summarize with α

$$\begin{array}{cc} Parallel & Series \\ \alpha = \dfrac{1}{2R_1C_1} & \alpha = \dfrac{R_1}{2L_1} \end{array} \quad (8)$$

and common ω_0,

$$\omega_0 = \frac{1}{\sqrt{L_1C_1}} \quad (9)$$

to give

$$\frac{d^2V_0}{d^2t} + 2\alpha\frac{dV_0}{dt} + \omega_0^2V_0 = 0 \qquad \frac{d^2I_0}{d^2t} + 2\alpha\frac{dI_0}{dt} + \omega_0^2I_0 = 0 \quad (10)$$

with final solution:

$$V_0 = A_1e^{S_1t} + A_2e^{S_2t} \qquad I_0 = A_1e^{S_1t} + A_2e^{S_2t} \quad (11)$$

where S_1 & S_2 for both parallel and series circuits are,

$$S_1 = -\alpha + \beta \quad (12)$$

$$S_2 = -\alpha - \beta \quad (13)$$

$$\boxed{\beta = \sqrt{\alpha^2 - \omega_0^2}}. \quad (14)$$

Thus the roots for the parallel circuits are,

$$S_{1(parallel)} = -\frac{1}{2R_1C_1} + \sqrt{\left(\frac{1}{2R_1C_1}\right)^2 - \frac{1}{L_1C_1}} \quad (15)$$

$$S_{2(parallel)} = -\frac{1}{2R_1C_1} - \sqrt{\left(\frac{1}{2R_1C_1}\right)^2 - \frac{1}{L_1C_1}} \quad (16)$$

and the roots for the series circuits,

$$S_{1(series)} = -\frac{R_1}{2L_1} + \sqrt{\left(\frac{R_1}{2L_1}\right)^2 - \frac{1}{L_1C_1}} \quad (17)$$

$$S_{2(series)} = -\frac{R_1}{2L_1} - \sqrt{\left(\frac{R_1}{2L_1}\right)^2 - \frac{1}{L_1C_1}}. \quad (18)$$

At this moment, great care should be taken to define the β criteria as shown in equation (14). On futher inspection, table 1 defines the results for the different type of oscillations. In this study, we are more interested in the imaginary result of β so that energy is stored at each cycle at a rate higher than consumed by resistance R.

Damped Oscillations	Criteria	β Result
Over	$\alpha^2 > \omega_0^2$	Positive
Critically	$\alpha^2 = \omega_0^2$	Zero
Under	$\alpha^2 < \omega_0^2$	Imaginary

Table 1: Damped Oscillations.

2.2 Principle of Resonance in Parametric Circuit

The serial resonance circuit (Fig. 2) represents a closed current loop consisting of an inductance L, a capacitance C, a resistor R and a voltage source U. It is a classical realization of a forced oscillation. According to Kirchhoff's law, the sum of the respective component voltages is equal to the driving voltage:

$$U_L + U_R + U_C = U. \tag{19}$$

The voltages of the components depend on the time-dependent current I and charge Q in the form

$$U_L = L\dot{I}, \tag{20}$$

$$U_R = RI, \tag{21}$$

$$U_C = \frac{Q}{C}. \tag{22}$$

where the dot is the time derivative. The current simply is

$$I = \dot{Q}. \tag{23}$$

Consequently we obtain the differential equation for a damped forced oscillation

$$L\ddot{Q}(t) + R\dot{Q}(t) + \frac{Q(t)}{C} = U(t) \tag{24}$$

where the quantities Q, I and U are time dependent, the others are constants. If a resonance circuit is excited by a pulse of U and then is left to its own resources, it performs damped oscillations where the total energy remains constant, as can be seen in Fig. 3.

Since the 1930's circuits have been studied [3] where some of the circuit elements are varying in time. Then Eq.(24) is not valid in general [4], it becomes a more complex differential equation with non-constant coefficients. Such equations are mostly not solvable analytically, therefore it was difficult at that time to predict the behavior of such circuits. Today these equations can simply be solved numerically by computer and parameter studies are possible easily.

As we will see the total energy is not conserved when parametric circuits are considered. We concentrate on one specific parametric circuit with a time-varying capacitance. We will see that this is the most simple design to produce excess energy. The basic definition of the charge in the capacitance (where Eq.(22) was derived from) reads

$$Q(t) = U_C(t)\ C(t) \tag{25}$$

i.e. the charge is not in proportion to the voltage. Formally Eq.(19) remains valid. There is no additional derivative because there was none in the defining

Eqs.(22) and (25) [1]. Practically, however, this means that with an oscillating capacitance the nature of the circuit is principally changed. There is an energy in- and outflow to be expected.

We specify the circuit further by a driving voltage

$$U(t) = U_0 \sin(\omega_0\ t) \tag{26}$$

and an oscillating capacitance

$$C_{eff}(t) = C\,(1 + a_0 \sin(\omega_1\ t + \varphi))\,, \quad a_0 < 1 \tag{27}$$

with a phase factor φ. The driving voltage and the capacitance have the same phase if $\varphi = 0,\ \ \omega_1 = n \cdot \omega_0$.

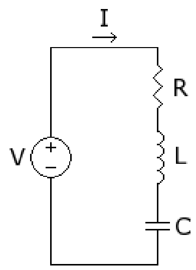

Figure 2: Serial resonance circuit with driving voltage [2].

3 Simulation Results

The design described in [3], [4] is investigated first by simulation. Then an alternative design is considered.

3.1 Design with Doubled Resonance Frequency

The simulation package OpenModelica [5] was applied to solve the time dependent equations. The following parameters were used for the circuit (in SI units):

$$\begin{aligned}
U_0 &= 5.0\ \text{V} && (28)\\
C &= 2.3 \cdot 10^{-7}\ \text{F} && (29)\\
L &= 0.02\ \text{H} && (30)\\
R &= 20\ \Omega && (31)\\
f_{res} &= \frac{1}{2\pi\sqrt{L\ C}} && (32)\\
\omega_0 &= 2\pi f_{res} && (33)\\
\omega_1 &= 2\ \omega_0 && (34)\\
a_0 &= 0.2 && (35)\\
\varphi &= 0 && (36)
\end{aligned}$$

[1] if we used a variable inductance for example, we had to use the equation $U_L(t) = \frac{d}{dt}(L(t)\ I(t))$ which leads to more terms according to the product rule.

According to [3], [4] we used a sinus-like capacitance variation with twice the resonance frequency (Eqs.(33, 34)). The behavior of the circuit was first checked by modeling a classical resonance circuit with $C = const$. The results show correctly that the current drops exponentially because of damping by the Ohmic resistance (Fig. 3(a)). Total energy is constant (Fig. 3(b)). After some time the whole energy of the oscillation being exchanged between the inductance and capacitance has been dissipated by the resistance. If this circuit is driven by a periodic voltage of the resonance frequency given by Eq.(32), the current amplitude becomes maximal, about 0.25 A (see Fig. 4(a)). We did not consider in Eq.(32) the shift of the resonance frequency by the resistance which changes this value slightly. From Fig. 4(b) it can be seen that after the oscillation has stopped the power loss (in Watts) is constant. This comes completely from the driving voltage U because energy is conserved.

The results differ totally as soon as the capacitance is made variable as described in Eq.(27). The current now grows unlimited (Fig. 5(a)) and so does the total energy. In Fig. 4(b) the dissipated power at the resistance is shown. In the range considered it increases to about 100 W effectively (that is half the peak values). The current amplitude of the resonant circuit with fixed capacitance is shown as the blue line in Fig. 5(a) for comparison. It can clearly be seen that the range of energy conservation is exceeded.

So far we drove the parametric circuit with the resonance frequency $f_{res} =$ 2346.6 Hz. In order to make technical use of this effect, the rising current must be limited, otherwise the circuit will be damaged within fractions of a second. Therefore sophisticated control electronics is required. However one can reduce this effort considerably by driving the circuit with a frequency slightly different from the resonance frequency. Using $f = 0.97 f_0$ which is only 3% below resonance, the current increases to an upper limit only, see Fig. 6(a). Consequently, the power loss remains finite, about 400 W effectively in the case considered (Fig. 6(b)).

So far we used a parametric capacitance with twice the frequency of the driving voltage and phase difference $\varphi = 0$. The phase shift can be optimized as shown in Figs. 7(a),7(b). It is at maximum for $\varphi = -\pi/2$. Since the power loss $P = I^2 R$ depends quadratically on the current I, it is even much higher in this case, amounting to about 1.5 kW effectively (Fig. 7(b)). Then the voltages at the inductance and capacitance are about 4000 V, which is technically feasible. With driving force of 5 V peak signal the current of 10 A flows through the voltage source, this could be considered as an input of 50 W compared to 4 kW peak output. This is a remarkable COP of 200. The proposed design is adequate for a small generator in households for example. The doubled frequency for the parametric capacitance was proposed in [3]- [4] and explained therein. Our simulations confirm this design.

3.2 Design with Original Resonance Frequency

Alternatively, we simulated configurations where the parametric frequency of the capacitance was identical to the resonance frequency:

$$\omega_1 = \omega_0. \tag{37}$$

Then the parametric signal must be pulse-like, a sinusoidal wave form does not produce the high COP in this case. We chose two waveforms, one with smooth spikes and a rectangular signal. In the former case we defined

$$C_{eff} = C\left(1 + a_0 \ \sin^7(\omega_1 t + \varphi)\right). \tag{38}$$

To obtain an increasing current, the frequency had to be chosen $f = 1.07 f_0$. The results are graphed in Figs. 8(a),8(b). The current grows exponentially. The parametric signal is shown Figs. 8(b), together with the charge Q which begins to oscillate in the time frame shown. Interestingly, the results were independent of the phase shift. The charge oscillation adopts itself so that the behavior shown in Fig. 8(b) occurs. It may be interpreted as a kind of "self-organization" which is sometimes reported in connection with systems of high COP.

The interpretation of this behavior is more obvious when a rectangular signal is used as shown in Fig. 9(a). While the capacitance is high (upper pulse region), the charge oscillation is increased. This can be seen from the fact that the amplitude in the upper half period is higher than in the preceding lower half period of Q. In the falling interval, Q goes down exactly to the negative of the positive amplitude value, there is no increase in this case. The second interval is shorter because the capacity is minimized here. In [4] the observed behavior has nicely been compared with a children's swing which is pushed on one side. The case with the doubled parametric frequency can be compared in this picture with the situation where the person stands on the swing and "hunkers down and up" during each half-period. The"hunkering down" appears with the doubled frequency of the swing.

Finally we observed another remarkable effect. The driving voltage can be switched off after one or two periods (Fig. 9(b)). It is even possible to omit the driving voltage completely and give a small current pulse or charge separation on the circuit initially. Then the oscillation of the capacitance is sufficient to start the circuit oscillation and bring the system in the high COP regime. This shows again that the system is self-organizing in a stable way. The results are in accordance with solution (17) where a series circuit not driven by an external source can show an ever increasing current. There is no energy input in this type of capacitor switching, except a small switching energy input which does not enter the calculation and will certainly be below 10 W while the output is about 2 kW. Insofar the COP is even higher than in the first design.

4 Conclusions

We have designed and simulated a solid state version of a mechanical parametric capacitor in a resonant circuit. The parametric switching can be realized by transistors, leading to a complete "solid state" design. One recommendation is to use Ideal MOSFET diodes for higher switching frequency, and other designs deserves further study. It's common knowledge that the higher the frequency the smaller the electrical components need to be; however, it is noted here that we lose the ability to handle higher power with smaller components. Nonetheless, the designs described in this article are good candidates to construct solid state renewable energy devices that shuttles energy from the time domain.

Driving the parametric elements in a non-linear form give us new and useful power as we saw from our simulations. Ide Osamu has also seen this effect in rate-of-change of magnetic flux by pulsing a transformer non-linearly [7], [8].

Analogously, driving a parametric capacitor non-linearly will give us a similar result but in the rate of change of electric flux.

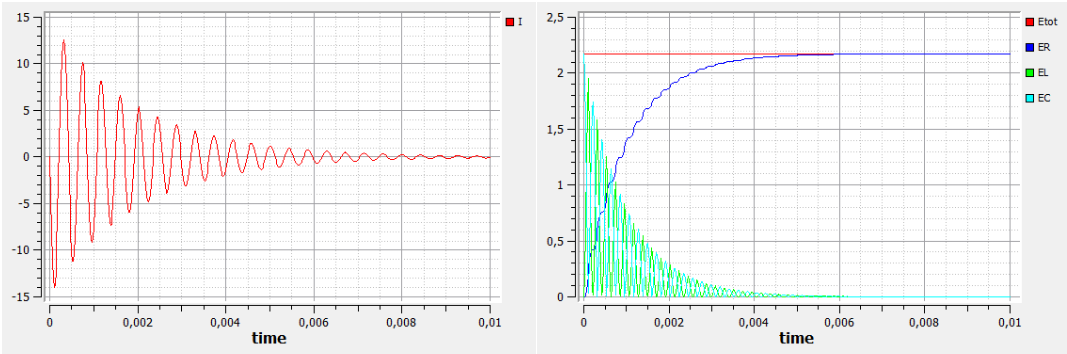

(a) Current (A) (b) Total energy (J)

Figure 3: (a) Current of a classical damped oscillator ciruit without external voltage.
(b) Total energy in a classical damped oscillator ciruit without external voltage, $E_{tot} = E_R + E_L + E_C$.

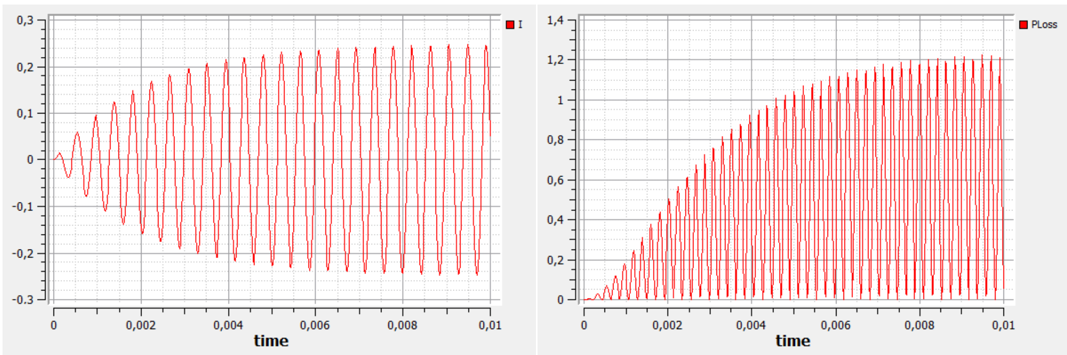

(a) Current (A) (b) Power loss (W)

Figure 4: Current (a) and dissipated power (b) in a classical damped oscillator ciruit with driving voltage at resonance.

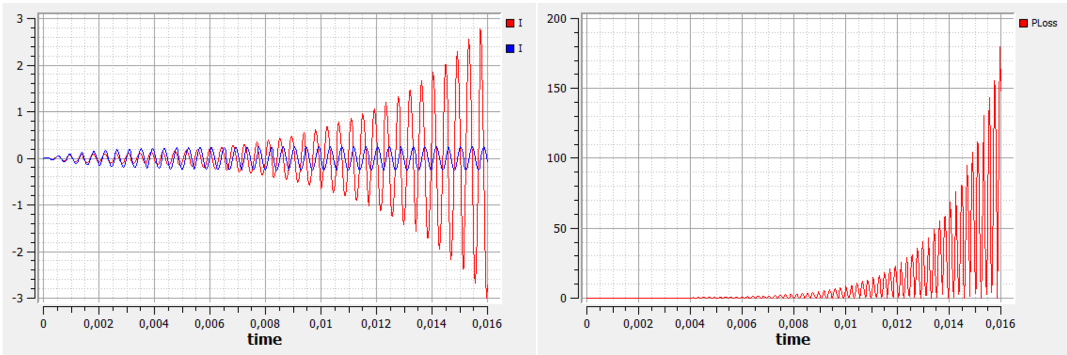

(a) Current (A) (b) Power loss (W)

Figure 5: (a) Current of the parametric circuit described by parameters of Eqs.(28-36). For comparison: current amplitude of the original free oscillating curcuit of Fig. 3a (blue curve).
(b) Dissipated power by the Ohmic resistance.

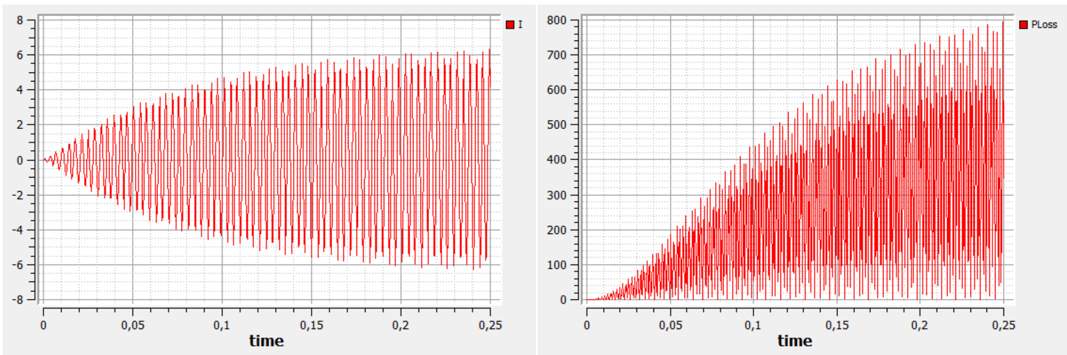

(a) Current (A) (b) Power loss (W)

Figure 6: Current (a) and dissipated power (b) of the parametric circuit for frequency $f = 0.97\ f_0$.

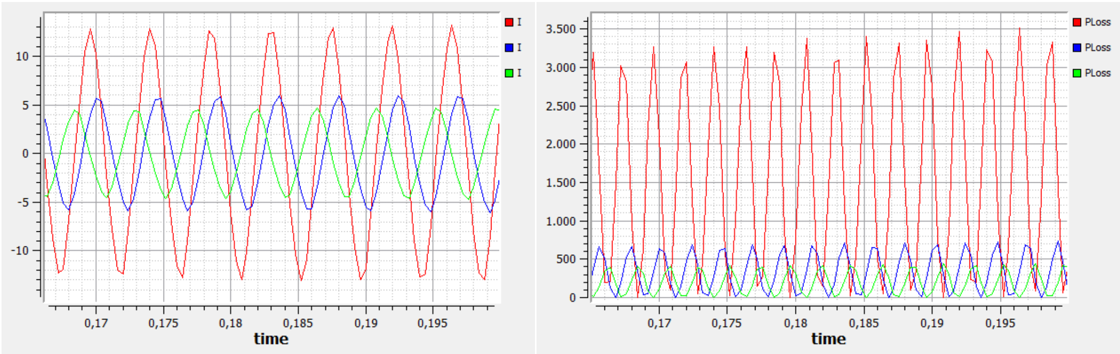

(a) Current (A)

(b) Power loss (W)

Figure 7: (a) Currents for different phase shifts between U and C_{eff} with $f = 0.97\ f_0$. red: $\varphi = -\pi/2$, blue: $\varphi = 0$, green: $\varphi = \pi/2$.
(b) Dissipated power for phase shifts of (a).

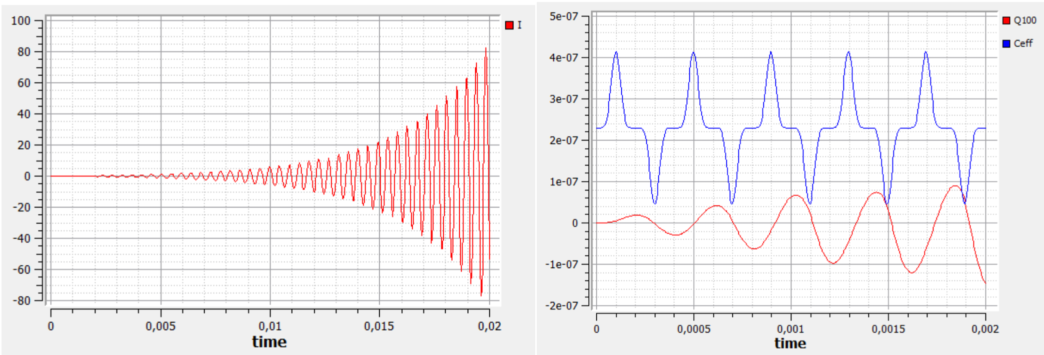

(a) Current (A)

(b) C_{eff} (F) and Charge Q/100 (C)

Figure 8: (a) Current for model with $\sin^7$ pulses, $f = 1.07\ f_0$, $\omega_1 = \omega_0$.
(b) C_{eff} and $Q/100$ for this model.

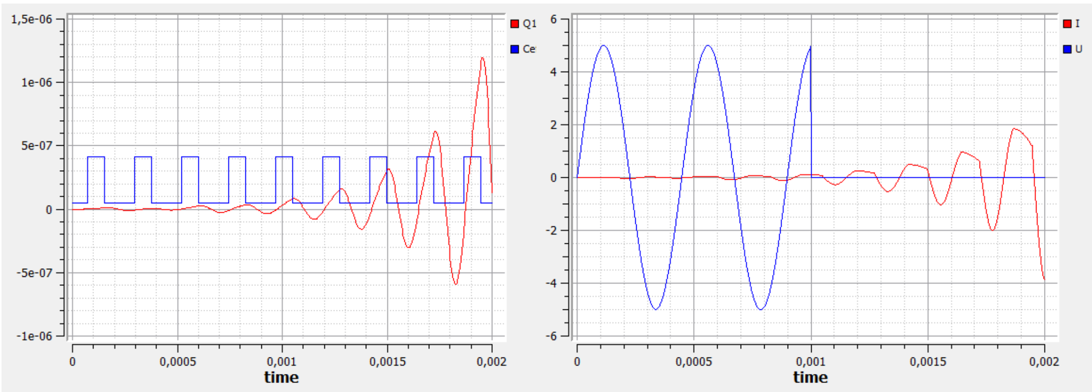

(a) C_{eff} (F) and Charge Q/100 (C)

(b) U (V), I (A)

Figure 9: (a) C_{eff} and $Q/100$ for model with rectangular pulses, $f = 0.95\ f_0$, $\omega_1 = \omega_0$.
(b) Interrupted driving voltage U and current I for this model.

References

[1] M. W. Evans et al., *Generally Covariant Unified Field Theory* (Abramis, Suffolk, 2005 onwards), vol. 1-7 (see also www.aias.us, section UFT papers).

[2] http://en.wikipedia.org/wiki/RLC_circuit.

[3] L. Mandelstam, N. Papalexi, A. Andronov, S. Chaikin and A. Witt, *Report on Recent Research on Nonlinear Oscillations*, NASA TT F-12,678, 20546, 1969. Translation of *Expose Des Recherches Recentes Sur Les Oscillations Non Lineaires*, Technial Physics of the USSR, Leningrad, Vol. 2, pp. 81-134, 1935.

[4] Yoshihisa Yamamoto, *NII Quantum Information Science, Leccture Notes Chapter 12, Parametric Amplifiers and Oscilaltors*, http://www.qis.ex.nii.ac.jp/qis/documents_YY/y3_02chp12_sld.pdf and http://www.qis.ex.nii.ac.jp/qis/documents_YY/y3_02chp12_txt.pdf.

[5] *OpenModelica open source simulation package with graphical user interface OMEdit*, version 1.8.0, http://www.openmodelica.org/.

[6] Kouril, F. & Vrba, K., *Non-Linear and Parametric Circuits: Principles, Theory and Applications*, Ellis Horwood Limited, 1st Ed, 1988, Ch 10.2.

[7] Osamu, Ide, *Increased voltage phenomenon in a resonance circuit of unconventional magnetic configuration*, J. Appl. Phys., Vol. 77, No. 11 (1 June 1995)

[8] Osamu, Ide, *Possibility of Existence of Non-Linear Electromotive Force (EMF)*, NASA/CP-2000-210291, Dec 1999. Fifth International Symposium on Magnetic Suspension Technology.

[9] Nahvi, M. & Edminister, J. *Schaum's Outline of Electric Circuits*, McGraw-Hill, 4th Ed., Dec. 2002., Ch 8.

[10] Maxwell, James Clerk, *On Mr. Grove's 'Experiment in Magneto-Electric Induction'. In a Letter to W.R.Grove, F.R.S*, Phil. Mag., vol. 35, pp.360-363; May, 1868. *Scientific Papers*, vol. 2, pp. 121-124

[11] Thomson, William, *On Transient Electric Currents*, Phil. Mag., vol. 5, pp.393-405; June, 1853. *Mathematical And Physical Papers*, vol. 1, pp. 540-553.

[12] Steinmetz, Charles Proteus, *Theory and Calculation of Alternating Current Phenomena*, Electrical World and Engineer, 3rd Ed., Jan. 1900, Ch. 21.

[13] Mandelstam, Von L. & Papalexi, N. *Uber die Erregung Von Eletrischen Schwingungen Durch Parameteraenderung*, J. Zeitschrift Fur, 1934.